

The New Acetaminophen Drug in the Form of Nano-Organometallic Compounds as a Bright Future for Antimicrobial Therapy

Abdou saad El-Tabl^{1*}, Moshira Mohamed Abd El-Wahed², Ahmed M. Ashour¹, Reham Ali S. Ahmed³

¹Department of Chemistry, El-Menoufia University, Shebin El-Kom, Egypt; ²Department of Pathology, El-Menoufia University, Shebin El-Kom, Egypt; ³Department of Forensic Toxicologist and Narcotics, Forensic Medicine Authority, Ministry of Justice, Egypt

ABSTRACT

New nano-organometallic compounds analogue to acetaminophen drug containing the same functional groups (hydroxyl (OH), amide (HN-CO-CH₃) and aromatic group (benzene ring)) have been prepared. They were characterized using elemental and advanced spectral techniques such as infrared and ultraviolet spectra, proton nuclear magnetic resonance, mass spectra, electron spin resonance and electron microscope as well as magnetism, conductivity and thermal analysis. The spectral and thermal data showed octahedral structure with stability of these compounds up to 50°C. The biological activity of the compounds against gram (+ve), gram (-ve) bacteria and fungi were carried out. Due to the difficulty of testing these compounds on animal viruses in our lab, we applied on plant viruses and impressive results were also obtained and this gave us hope for applying it to human viruses for example corona virus. The order of activity was, for gram +ve (staphylococcus aureus): Cd(II) compound (3)>Co(II) compound (6)>Ampicillin>Ni(II) compound (4)>Cu(II) compound (5)>Cu(II) compound (2)>Zn(II) compound (7)>acetaminophen=ligand (organic compound). For gram -ve Escherichia coli, the order was Cd(II) compound (3)>Ampicillin> Co(II) compound (6)> Ni(II) compound (4)>Cu(II) compound (5)>Cu(II) compound (2)>Zn(II) compound (7)>acetaminophen=ligand (organic compound). For (Aspergillus flavus), the order was Cd(II) compound (3)>Amphotericin B>acetaminophen=ligand (organic compound)=Cu(II) compound (2)=Ni(II) compound (4)=Cu(II) compound (5)=Co(II) compound (6)=Zn(II) compound (7) and for Candida albicans, the order was Cd(II) compound (3)>Amphotericin>Ni(II) compound (4)>Co(II) compound (6)>Cu(II) compound (5)>Cu(II) compound (2)>acetaminophen=ligand (organic compound)=Zn(II) compound (7). The above results showed Cd(II) compound (3) is the highest potent against gram (+ve), gram (-ve) and fungi compared to standard drugs. Cytotoxic effect of this compound was carried out on experimental rats and no toxic effects were observed (six months) on the functions of all organs using clinical analyses.

Keywords: Nano-organometallic compounds; Elemental and spectral analyses; Biological activity

INTRODUCTION

Acetaminophen (an international name used in the USA) is derived from its chemical name N-acetyl-para-aminophenol. This drug has a long history and, as it often happens with important discoveries, it was found by chance. Acetaminophen is one of the most popular and most commonly used analgesic and antipyretic drugs around the world, available without a prescription, both in mono- and multi-component preparations [1-5]. It is the drug of choice in patients that cannot be treated with Non-Steroidal Anti-Inflammatory Drugs (NSAID), such as people with bronchial asthma, peptic ulcer disease, hemophilia, salicylate-sensitized people, Children under 12 years of age, pregnant or breastfeeding women [6-8]. It is recommended as a first-line treatment of pain

associated with osteoarthritis. The mechanism of action is complex and includes the effects of both the peripheral (COX inhibition), and central (COX, serotonergic descending neuronal pathway, L-arginine/NO pathway, cannabinoid system) antinociception processes and "redox" mechanism. Nanotechnology refers to the creation and utilization of materials whose constituents exist at the nanoscale and by convention, be up to 100 nm in size [9]. Nanotechnology explores electrical, optical, and magnetic activity as well as structural behavior at the molecular and sub-molecular level. It has the potential to revolutionize a series of medical and biotechnology tools and procedures so that they are portable, cheaper, safer, and easier to administer [10]. Due to their exceptional properties including antibacterial activity, high resistance to oxidation and high thermal conductivity, nanoparticles have

Correspondence to: Abdou saad El-Tabl, Department of Chemistry, Faculty of Science, El-Menoufia University, Shebin El-Kom, Egypt, Tel: 01003313656; E-mail: asaeltabl@yahoo.com

Received: December 28, 2020; **Accepted:** January 11, 2021; **Published:** January 18, 2021

Citation: El-Tabl AS, Abd El-Wahed MM, Ashour AM, Ahmed RAS (2021) The New Acetaminophen Drug in the Form of Nano-Organometallic Compounds as a Bright Future for Antimicrobial Therapy. Drug Des. 10:174.

Copyright: © 2021 El-Tabl AS, et al. This is an open-access article distributed under the terms of the Creative Commons Attribution License, which permits unrestricted use, distribution, and reproduction in any medium, provided the original author and source are credited.

attracted considerable attention in recent years. Nanoparticles in the form of organometallic compounds can be synthesized chemically or biologically. Viruses are infectious agents that affect cells of almost all types of organisms. They are the smallest and simplest of all the microbes [11-15]. All viruses contain DNA or RNA. This genetic material is enclosed by a protein shell called a capsid. Many viruses also have an outer membrane surrounding them. Most viruses are shaped like rods or spheres. However, some viruses have a very unique appearance. Viruses need a host cell to reproduce. The virus will invade a healthy cell and use it to make more viruses. The host cell is usually killed in this process. Once inside the host cell, the virus injects its DNA (RNA) into the cell. The viral DNA takes control and makes copies of itself leading to more and more viruses. The new viruses then burst out of the cell and invade others, over and over. Most viruses cannot be treated. A person's immune system must fight it without the typical help of medicines. However, vaccines (immunizations you can get in order to prevent a virus from invading your cells and making you sick) and some anti-viral drugs may be used to control or prevent the spread of viral diseases. Viral diseases are among the most widespread illnesses in humans [16-18]. These illnesses range from mild fevers to some forms of cancer and include several other severe and fatal diseases. Transmission of these illnesses varies. Some are transmitted by human contact, while others are transmitted through water, an insect bite or are airborne. In this manuscript, new nano-organometallic compounds analogue to acetaminophen drug have been prepared and characterized using elemental and spectroscopic methods. Antimicrobial activity of these compounds has been studied as well as cytotoxic effect on experimental rats [19-21].

MATERIALS AND METHODS

Materials

The starting chemicals were of analytical grade and used without further purification.

Physical and spectroscopic techniques

The characterization of the ligand and its compounds carried out using various spectroscopic techniques such as: Elemental analyses (C, H, N and Cl) were performed by analytical laboratory of Cairo University, Egypt.

Molar conductivity

The molar conductivity of 10^{-3} M of compounds in dimethylsulfoxide (DMSO) was determined using Bibby conductimeters MCI at room temperature. Molar conductivities were calculated according to the following equation:

$$\Lambda^m = V * K * g / Mw * \Omega$$

Where: Λ^m =molar conductivity ($\text{ohm}^{-1}\text{cm}^2\text{mol}^{-1}$)

V=volume of the solution (100 cm^3)

K=cell constant: 0.92 cm^{-1}

Mw=molecular weight of the complex

g=grams of complex dissolved in 100 cm^3 solution

Ω =resistance measured in ohms.

Mass spectra

The mass spectra of the compounds were recorded on JEOL JMS-XA-500 mass spectrometer.

Thermal analyses

DTA and TGA were carried out on a Shimadzu DT-30 thermal analyzer in nitrogen atmosphere, from room temperature to 600°C at a heating rate of 10°C per minute.

$^1\text{H-NMR}$ spectra

The $^1\text{H-NMR}$ spectra were recorded on a JEOL EX-270 MHZ FT-NMR spectrometer in deuterated dimethylsulfoxide (DMSO-d_6) as a solvent. The chemical shifts were measured relative to the solvent peaks.

IR spectra

The infrared spectra of the ligand and its compounds were recorded on Perkin Elmer's infrared spectrometer 681 using KBr or CsBr discs.

Electronic absorption spectra

The electronic absorption spectra of the compounds were recorded on UNICO SQ-4802 UV/Vis. Double beam spectrophotometer ($190\text{-}1100 \text{ nm}$) using 1 cm quartz cell using DMSO as a solvent.

Magnetic susceptibility

The magnetic susceptibilities of the solid compounds in the solid state were measured in a borosilicate tube with a Johnson Matthey [8] at room temperature using the following equations:

$$X_a = \frac{2.086L(R - R^\circ)}{109W}$$

$$X_m = X_a * Mw$$

$$X_n = X_m - D$$

$$\mu_{\text{eff}} = 2.828(X_n \times T)^{1/2}$$

Where

X_a =mass susceptibility; L=sample length in cm; R=tube+sample reading; R° =empty the reading; W=mass of the sample; X_m =molar susceptibility; Mw=molecular weight; X_n =corrected molar susceptibility; D=diamagnetic corrections; μ_{eff} =effective magnetic moment; T=room temperature in Kelvin.

Determination of metal content

Metal content was determined using colorimetric method on HACH DR 5000 spectrophotometer [22-24].

ESR spectra

The solid ESR spectra of some compounds were recorded with ELEXSYS E500 Bruker spectrometer in 3 nm Pyrex Tubes at 25°C . Diphenylpicrylhydrazide (DPPH) free radical was used as a g-marker for the calibration of the spectra. The equation used to determine g-values was $g = (g_{\text{DPPH}})(H_{\text{DPPH}})/H$ Where: $g_{\text{DPPH}} = 2.0036$; H_{DPPH} =magnetic field of DPPH in gauss; H=magnetic field of the sample in gauss.

Preparation of the ligand (1)

It was prepared by refluxing with stirring for two hours of p-hydroxy-methyl benzoate (10.0 g , 1.914 mol) with o-phenylene diamine (6.2 g , 1.913 mol) in 30 cm^3 ethanol. The solid product which formed left to cool at room temperature, filtered off, washed with ethanol and dried in air. The solid hydriized p-hydroxy-benzoic-1,2-phenylene diamine (15.0 g , 0.188 mol) dissolved in 35 cm^3 ethanol, acetic anhydride (6.7 g , 0.187 mol) was added. Reflux the mixture with stirring for another two hours and then left the product to

cool at room temperature, filtered off the formed precipitate and leave it to dry at room temperature. Recrystallize the product in ethanol and dried to give the final organic ligand.

Preparation of ligand (1) is shown in Figure 1.

The mass spectrum of the ligand (H_2L) revealed molecular ion peak at m/z 270. Analytical data for ligand (1) and its compounds are given in Table 1.

Preparation of organometallic compounds (2)-(7)

The metal compounds (2)-(7) were prepared by refluxing with stirring a suitable amount of a hot ethanolic solution (30 cm^3) of the following metal salts: $Cu(OAc)_2 \cdot H_2O$ (0.29 g, 0.053 mol)

compound (2), $Cd(OAc)_2 \cdot 4H_2O$ (0.349 g, 0.054 mol) compound (3), $Ni(OAc)_2 \cdot 4H_2O$ (0.399 g, 0.0534 mol) compound (4), $CuSO_4 \cdot 5H_2O$ (0.358 g, 0.0534 mol) compound (5), $CoSO_4 \cdot 7H_2O$ (0.450 g, 0.0534 mol) compound (6), $Zn(NO_3)_2 \cdot 4H_2O$ (0.304 g, 0.0533 mol) compound (7), with a hot ethanolic solution of the ligand (1) (0.5 g, 0.0534 mol) in 30 cm^3 ethanol for 1-3 hours range depending on the anion used. The precipitates which formed were filtered off, washed with ethanol then by diethyl ether and dried in vacuum desiccators over P_4O_{10} . The analytical and physical data are shown in Table 1.

Biological activity

Antimicrobial activity: Antimicrobial activity of the tested compounds was assessed against gram positive bacteria (*Staphylococcus aureus*), gram negative bacteria (*Escherichia coli*) and fungi (*Aspergillus flavus*) and (*Candida albicans*) using disc diffusion method [25]. Standard discs of Ampicillin (Antibacterial agent), Amphotericin B (Antifungal agent) served as positive controls for antimicrobial activity. The test compounds were dissolved in DMSO to give concentrations 250, 200, 175, 150 and 125 ppm and a DMSO poured disc was used as negative control. The bacteria were subcultured in nutrient agar medium, which was prepared using peptone, beef extract, NaCl, agar and distilled water. The Petri dishes were incubated for 48 hours at 37°C. The standard antibacterial drug tetracycline was also screened under similar conditions for comparison. The zone of inhibition was measured in millimeters carefully. All determination was made in duplicate for each of the compounds. An average of the two independent readings for each compound was recorded.

Antivirsus activity: Nano-Cd(II) compound (3) has been prepared in concentration 1×10^5 ml mol/L (DMF/Saline). Compound spray is used for two successive days with good coverage of infected leaf surface including young, recently unfolded leaves. After one week, we photographed the infected plant without treatment with the compound and plant that was sprayed with the compound.

RESULTS AND DISCUSSION

The ligand (1) and its metal compounds (2)-(7) are stable at room temperature, non-hygroscopic and are insoluble in common solvents such as ethanol, acetone, water and chloroform but soluble

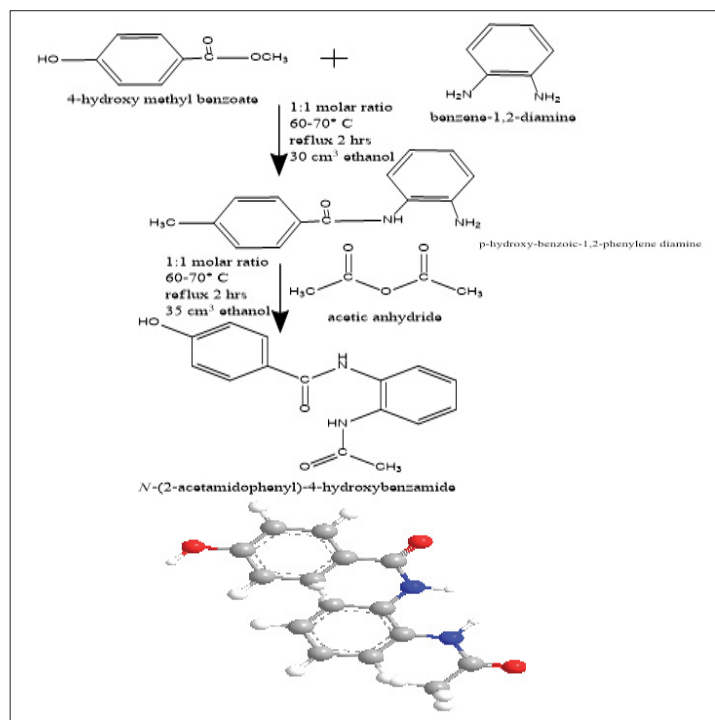


Figure 1: Ligand (1) Yield 91%; melting point: 70; color is dark brown; Anal. Calcd. For $C_{15}H_{14}N_2O_3$ (FW=270): C: 66.6; H: 5.2; N: 10.37. Found (%) C: 66.3; H: 5.1; N: 10.22; IR (KBr, cm^{-1}), 3367 ν (OH), 3288 ν (NH), 1680, 1685 ν (C=O), 1279 ν (C-OH); the mass spectrum of the ligand (H_2L) revealed molecular ion peak at m/z 270.

Table 1: Analytical and physical data of the ligand 1 and nano-metal compounds.

S. No.	Ligand/compounds	Color	FW	M.P (°C)	Yield (%)	Anal./Found (Calc.) (%)				Conductivity Λ
						C	H	N	M	
1	[HL] $C_{15}H_{14}N_2O_3$	Dark brown	270	70	91	66.3 (66.6)	5.1 (5.2)	10.22 (10.37)	-	-
2	[(HL) $Cu(OAc)_2(H_2O)] \cdot 1.2H_2O$ $C_{19}H_{26}CuN_2O_{10}$	Black	505.5	88	92	45.22 (45.1)	5.13 (5.1)	5.55 (5.5)	12.75 (12.5)	4.3
3	[(HL) $Cd(OAc)_2(H_2O)] \cdot 1.2H_2O$ $C_{19}H_{26}CdN_2O_{10}$	Brown	554.5	84	70	41.35 (41.1)	4.7 (4.6)	5.01 (5.05)	20.33 (20.2)	5
4	[(HL) $Ni(OAc)_2(H_2O)] \cdot 1.2H_2O$ $C_{19}H_{26}NiN_2O_{10}$	Light green	507.39	93	85	44.66 (44.9)	5.13 (5.1)	5.53 (5.5)	11.67 (11.55)	4.1
5	[(HL) $Cu(SO_4)(H_2O)_2] \cdot 1.2H_2O$ $C_{15}H_{22}CuN_2O_{11}S$	Black	501.5	92	89	35.87 (35.9)	4.47 (4.4)	5.62 (5.6)	12.92 (12.7)	7
6	[(HL) $Co(SO_4)(H_2O)_2] \cdot 1.2H_2O$ $C_{15}H_{22}CoN_2O_{11}S$	Black	496.9	95	79	36.29 (36.2)	4.53 (4.4)	5.49 (5.6)	11.97 (11.6)	6.5
7	[(HL) $Zn(NO_3)_2(H_2O)] \cdot H_2O$ $C_{15}H_{18}ZnN_4O_{11}$	orange	495.3	80	68	36.99 (36.3)	3.69 (3.6)	11.66 (11.3)	13.39 (13.2)	4.8

Note: $^*m^{-1}cm^2mol^{-1}$

in DMF and DMSO. The compounds are in nano-form and stable up to 50°C. The elemental analysis confirmed that, all compounds are composed of the ligand and metal ions with molar ratio equal to 1L:1M. Many attempts were made to grow a single crystal, but unfortunately, they failed until now. Organo-metallic compounds are found in nano form having size range from (5.68-9.47) make different properties of these compounds. The analytical, physical and spectral data are presented in Tables 1-6 which are compatible with the suggested structures as shown in Figure 2. Electron microscopic image of compound (3) is showed in Figure 3.

The molar conductivity

The molar conductivities of 1×10^{-3} M solutions of the compounds in DMSO at room temperature were found in the range 4.3-7.0 ohm⁻¹ cm² mol⁻¹ indicating the non-electrolytic in nature of all compounds. These low values commensurate the coordination of the anions to the metal ions [24-26].

Mass Spectra of the Ligand [H₂L], (1) and some of its nano-metal compounds

The mass spectrum of ligand [H₂L], (Table 2a) showed the molecular ion peak at m/z 270 amu, confirming its formula weight (F.W. 270). The mass fragmentation patterns observed at m/z=52, 65, 77, 93, 121, 132, 200 and 270 amu correspond to C₃H₂N, C₄H₃N, C₅H₃N, C₅H₃NO, C₆H₃NO₂, C₆H₁₄NO₂, C₉H₁₆N₂O₃ and C₁₅H₁₄N₂O₃ moieties, respectively, supported the suggested structure of the ligand.

The mass spectrum of compound (2) (Table 2b) showed the

Table 2a: Mass spectrum of the ligand 1.

Ligand	m/z	Rel. Int.	Fragment
Ligand 1	52	20	C ₃ H ₂ N
	65	55	C ₄ H ₃ N
	77	18	C ₅ H ₃ N
	93	15	C ₅ H ₃ NO
	121	76	C ₆ H ₃ NO ₂
	132	100	C ₆ H ₁₄ NO ₂
	200	18	C ₉ H ₁₆ N ₂ O ₃
	270	15	C ₁₅ H ₁₄ N ₂ O ₃

Table 2b: Mass spectrum of the compound 2.

Compound	m/z	Rel. Int.	Fragment
Compound 2	53	18	C ₃ HO
	60	96	C ₃ H ₈ O
	80	27	C ₃ H ₁₂ O ₂
	93	20	C ₄ H ₁₃ O ₂
	108	51	C ₄ H ₁₄ NO ₂
	121	100	C ₅ H ₁₅ NO ₂
	152	39	C ₅ H ₁₆ N ₂ O ₃
	192	27	C ₈ H ₂₀ N ₂ O ₃
	310	25	C ₁₁ H ₂₂ N ₂ O ₄ Cu
	326	34	C ₁₁ H ₂₂ N ₂ O ₅ Cu
	368	38	C ₁₃ H ₂₄ N ₂ O ₆ Cu
	438	26	C ₁₆ H ₂₆ N ₂ O ₈ Cu
	505	25	C ₁₉ H ₂₆ N ₂ O ₁₀ Cu

molecular ion peak at m/z 505 amu, confirming its formula weight (F.W. 505). The mass fragmentation patterns observed at m/z=53, 60, 80, 93, 108, 121, 152, 192, 310, 326, 368, 438 and 505 amu correspond to C₃HO, C₃H₈O, C₃H₁₂O₂, C₄H₁₃O₂, C₄H₁₄NO₂, C₅H₁₅NO₂, C₅H₁₆N₂O₃, C₈H₂₀N₂O₃, C₁₁H₂₂N₂O₄Cu, C₁₁H₂₂N₂O₅Cu, C₁₃H₂₄N₂O₆Cu, C₁₆H₂₆N₂O₈Cu and C₁₉H₂₆N₂O₁₀Cu moieties, respectively, supported the suggested structure of the compound.

However, the mass spectrum of the compound (7) (Table 2c) showed the molecular ion peak at m/z 495 amu, confirming its formula weight (F.W. 495). The mass fragmentation patterns observed at m/z=54, 66, 80, 92, 108, 121, 133, 150, 163, 192, 236, 279, 300, 319, 402, 456, 480 and 495 amu correspond to C₃H₂O, C₄H₂O, C₄H₂NO, C₅H₂NO, C₅H₂NO₂, C₆H₃NO₂, C₇H₃NO₃, C₇H₄NO₃, C₈H₅NO₃, C₈H₆N₃O₃, C₉H₆N₃O₅, C₁₀H₆N₃O₇, C₁₀H₁₁N₃O₈, C₁₀H₁₄N₃O₉, C₁₀H₁₆N₃O₁₀Zn, C₁₂H₁₆N₄O₁₁Zn, C₁₄H₁₆N₄O₁₁Zn, and C₁₅H₁₈N₄O₁₁Zn moieties, respectively, supported the suggested structure of the compound.

IR spectra

The IR spectra of the ligand (1) showed a strong vibration band located at 1685 cm⁻¹ which assigned to the carbonyl ν(C=O) of the acetyl group, whereas the weak and broad bands which observed at 3467 and 3288 cm⁻¹ are assigned to the stretching vibrations of the aromatic hydroxyl and ν(NH) groups. The broad bands appeared at 3560-3170 and 3160-2600 cm⁻¹ ranges are assigned to inter- and intramolecular hydrogen bondings [27-31]. These observations confirmed the presence of the ligand in the ketonic form in the solid state [29-34]. The spectrum of the ligand also showed band at 1625 cm⁻¹ which may be assigned to keto of amide ν(C=O) groups [32]. By comparing the IR spectral data of the nano-compounds with that of the free ligand. It is noted that, in all compounds the appearance of a new band in the range of 1678-1670 cm⁻¹ which may be assigned to the C=O acetyl group and this band shifted to lower value confirming coordination of this group to the metal ion [31]. In the spectra of all compounds, the absorption frequency of amide carbonyl group ν(C=O) was shifted to lower frequency side and appeared in the region 1614-1607 cm⁻¹ range

Table 2c: Mass spectrum of the compound 7.

Compound	m/z	Rel. Int.	Fragment
Compound 7	54	19	C ₃ H ₂ O
	66	24	C ₄ H ₂ O
	80	43	C ₄ H ₂ NO
	92	22	C ₅ H ₂ NO
	108	100	C ₅ H ₂ NO ₂
	121	20	C ₆ H ₃ NO ₂
	133	33	C ₇ H ₃ NO ₃
	150	20	C ₇ H ₄ NO ₃
	163	23	C ₈ H ₅ NO ₃
	192	18	C ₈ H ₆ N ₃ O ₃
	236	22	C ₉ H ₆ N ₃ O ₅
	279	15	C ₁₀ H ₆ N ₃ O ₇
	300	15	C ₁₀ H ₁₁ N ₃ O ₈
	319	12	C ₁₀ H ₁₄ N ₃ O ₉
	402	18	C ₁₀ H ₁₆ N ₃ O ₁₀ Zn
	456	16	C ₁₂ H ₁₆ N ₄ O ₁₁ Zn
480	15	C ₁₄ H ₁₆ N ₄ O ₁₁ Zn	
495	12	C ₁₅ H ₁₈ N ₄ O ₁₁ Zn	

with lowering its intensity confirmed the coordination of oxygen atom of amide $\nu(\text{C}=\text{O})$ with the metal ions without undergoing enolization. Also, it was observed that, the presence of absorption band due to hydroxyl group which appeared in the spectra of compounds at 3465-3450 cm^{-1} range indicated that, this group is not coordinated to the metal ion Table 3 [35]. The appearance of new bands appeared in the ranges 626-605, and 565-505 cm^{-1} ranges for different compounds may be assigned to the $\nu(\text{M}-\text{O})$, and $\nu(\text{M}-\text{N})$, respectively [30-37]. These results confirmed that, the bonding of the ligand with the metal ions occurred via carbonyl oxygen of acetyl and amide group and NH nitrogen atom [38]. In the case of acetate compounds (2)-(4) there are two new bands appeared in the 1443-1440 and 1315-1314 cm^{-1} ranges which are attributed to the symmetric and asymmetric stretching vibration of the acetate group. The separation values (Δ) between $\nu_{\text{sym}}(\text{COO}^-)$ and $\nu_{\text{asym}}(\text{COO}^-)$ in these compounds suggesting the coordination of acetate group in as a monodentate fashion [39,40]. In the case of sulfate compounds (5) and (6), there are new bands appeared in the 1234-1231, 1164-1100 and 697-688 ranges for the complexes, respectively. These bands indicate that, the sulfate ion is coordinated to the metal ion. Compound (7) showed bands at 1373, 1235, 800 and 697 cm^{-1} indicating coordination of nitrate group to the metal ion in unidentate fashion [38-42]. The above results together with elemental analyses indicate that, the ligand behaved as neutral tridentate fashion bonded to the metal ions through carbonyl oxygen atoms of acetyl and amide and NH groups [39-47].

Magnetic moments

The magnetic moments of the nano-metal compounds (2)-(7) at room temperatures are shown in Table 4. Cu(II) compounds (2)

and (5) show values at 1.71 and 1.69 B.M corresponding to one unpaired electron in the $d_{(x^2-y^2)}$ ground state in an octahedral structure. The low values than 1.73 B.M is due to spin - spin interactions takeplace between Cu(II) ions [43-48]. Cd(II) complex (3) Zn(II) compound (7) showed diamagnetic property [53-56]. Ni(II) compound (4) showed value equal to 2.93 B.M. The lowering in the value may be assigned to the interaction between the two nickel atoms via hydrogen bondings or molecular association [43-49]. The magnetic moment of Co(II) compound (6) equal to 4.75 B.M, indicating octahedral structure [50-52].

Electronic spectra

The electronic spectral data for the ligand (1) and their metal compounds in DMSO are summarized in Table 4. The electronic absorption spectra of the ligand showed three bands located at 295, 315 and 335 nm respectively. The first one assigned to intraligand $\pi \rightarrow \pi^*$ transition in the hydroxyl moiety which is nearly unchanged on complexation. The second and third bands may be assigned to $n \rightarrow \pi^*$ and charge transfer transitions of the NH and carbonyl groups. The location of these bands was found to be shifted to higher energy on complexation. This finding indicated to the participation of these groups in bonding and coordination with metal ions [28,46]. Copper(II) compounds (2), and (5) showed bands in the 318-280, 475-450, 590-575 and 610-608 nm ranges, were assigned to intraligand transition $\text{O} \rightarrow \text{Cu}$, charge transfer, ${}^2\text{B}^1 \rightarrow {}^2\text{E}$ and ${}^2\text{B}^1 \rightarrow {}^2\text{B}^2$ transitions, indicating a distorted octahedral structure [57-59]. The electronic spectrum nickel(II) compound (4) showed bands at 288, 310, 320, 462, 570, 610 and 740 nm, which are assignable to intraligand transition ${}^3\text{A}_{2g}(\text{F}) \rightarrow {}^3\text{T}_{1g}(\text{p})$ (3), ${}^3\text{A}_{2g}(\text{F}) \rightarrow {}^3\text{T}_{1g}(\text{F})$ (3) and ${}^3\text{A}_{2g}(\text{F}) \rightarrow {}^3\text{T}_{1g}(\text{F})$ (3) transitions respectively, assuming the octahedral Ni(II) compound [54,55]. The (ν_2/ν_1)

Table 3: IR frequencies of the bands (cm^{-1}) of the ligand 1 and its nano-metal compounds.

S. No.	$\nu(\text{H}_2\text{O})$	$\nu(\text{OH})$	$\nu(\text{H-bonding})$	$\nu(\text{C}=\text{O})$ Acetyl	$\nu(\text{C-OH})$	$\nu(\text{C}=\text{O})$ Amide	$\nu(\text{NH})$	$\nu(\text{Ar})$	$\nu(\text{OAc})/\text{SO}_4/\text{NO}_3$	$\nu(\text{M-O})$	$\nu(\text{M-N})$
1	-	3467	(3560-3170), (3160-2600)	1685	1279	1625	3288	(1550, 1511), (850, 748)	-	-	-
2	(3470-3270), (3260-3100)	3460	(3560-3210), (3200-2750)	1670	1279	1607	3273	(1540, 1520), (851, 769)	1442, 1315	626	560
3	(3460-3290), (3240-3110)	3450	(3540-3200), (3180-2740)	1671	1280	1610	3270	(1538, 1518), (852, 768)	1443-1315	618	561
4	(3450-3280), (3240-3105)	3455	(3550-3220), (3190-2760)	1671	1279	1606	3265	(1536, 1517), (852, 767)	1440-1314	620	556
5	(3528-3313), (3300-3105)	3450	(3573-3200), (3190-2777)	1678	1280	1614	3290	(1532, 1514), (851, 769)	(1231,1159), (1110,697)	613	562
6	(3520-3320), (3310-3115)	3465	(3571-3205), (3195-2782)	1674	1279	1612	3284	(1533, 1516), (849, 765)	(1234,1164), (1100,688)	610	561
7	(3500-3325), (3315-3175)	3460	(3505-3190), (3180-2705)	1674	1277	1614	3255	(1531,1518), (852,769)	(1373,1235), (800,697)	611	561

Table 4: The electronic absorption spectral bands (nm) and magnetic moments (B.M.) for the ligand 1 and its nano-compounds.

S. No.	λ_{max} (nm)	μ_{eff} in B.M.	ν_2/ν_1
1	295 nm (log ϵ =3.98), 315 nm (log ϵ =4.25) 335(log ϵ =4.59)	-	-
2	280, 305, 315, 450, 590, 000	1.71	-
3	290, 310, 320	Diamagnetic	-
4	288, 310, 320, 462, 570, 610, 740	2.93	1.56
5	287, 302, 318, 475, 575, 608	1.69	-
6	292, 305, 315, 435, 562, 610	4.75	-
7	298, 305, 325	Diamagnetic	-

ratio for the compound was less than the usual value 1.6 indicating distorted octahedral Ni(II) compound, the (v_2/v_1) value equal to 1.56, indicating distorted octahedral structure. The electronic spectrum of Co(II) compound(6) showed bands at 292, 305, 315, 435, 562 and 610 nm. The first three bands are within the ligand and indicating intraligand transition. However, the other bands are due to ${}^4T_{1g}(F) \rightarrow {}^4T_{2g}(p)$, ${}^4T_{1g}(F) \rightarrow {}^4A_{2g}(F)$, ${}^4T_{1g}(F) \rightarrow {}^4T_{2g}(F)$, transition respectively, indicating distorted octahedral structure around the Co(II) ion [60]. Cd(II) compound (3) and Zn(II) compound (7) showed bands were due to t^0 intraligand transitions.

Electron Spin Resonance (ESR)

The ESR spectral data for copper (II) compounds (2) and (5) were presented in Table 5. The spectra of copper(II) compounds were characteristic of species d^9 configuration having axial type of a $d_{(x^2-y^2)}$ ground state which is the most common for copper(II) compounds. The compounds showed $g_{\parallel} > g_{\perp} > 2.0023$, indicating octahedral geometry around copper(II) ion. The g -values are related by the expression $G = (g_{\parallel} - 2) / (g_{\perp} - 2)$, where (G) exchange coupling interaction parameter (G). If $G < 4.0$, a significant exchange coupling is present, whereas if G value > 4.0 , local tetragonal axes are aligned parallel or only slightly misaligned. Copper(II) compounds showed 3.00 and 2.70 values indicating spin-exchange interactions takeplace between copper(II) ions. This phenomenon is further confirmed by the magnetic moments values Table 4. The $g_{\parallel}/A_{\parallel}$ value is also considered as a diagnostic term for stereochemistry, the $g_{\parallel}/A_{\parallel}$ values are 155.7 and 182.5 which are expected for distorted octahedral compounds [60-64]. The g -values of the copper(II) compounds with a ${}^2B_{1g}$ ground state ($g_{\parallel} > g_{\perp}$) may be expressed by

$$g_{\parallel} = 2.002 - (8K_{\parallel}^2 / \Delta E_{xy}) \quad (1)$$

$$g_{\perp} = 2.002 - (2K_{\perp}^2 / \Delta E_{xz}) \quad (2)$$

Where k_{\parallel} and k_{\perp} are the parallel and perpendicular components respectively of the orbital reduction factor (K), is the spin-orbit coupling constant for the free copper, ΔE_{xy} and ΔE_{xz} are the electron transition energies of ${}^2B_{1g} \rightarrow {}^2B_{2g}$ and ${}^2B_{1g} \rightarrow {}^2E_g$. From the above relations, the orbital reduction factors (K_{\parallel} , K_{\perp} , K), which are measure terms for covalency, can be calculated. For an ionic environment, $K=1$; while for a covalent environment, $K < 1$. The lower the value of K , the greater is the covalency.

$$K^2_{\perp} = (g_{\perp} - 2.002) \Delta E_{xz} / 2_0 \quad (3)$$

$$K^2_{\parallel} = (g_{\parallel} - 2.002) \Delta E_{xy} / 8_0 \quad (4)$$

$$K^2 = (K_{2\parallel} + 2K^2_{\perp}) / 3 \quad (5)$$

K values for the copper(II) compounds are indicating for a covalent bond character. Kivelson and Neiman noted that, for ionic environment $g_{\parallel} \geq 2.3$ and for a covalent environment $g_{\parallel} < 2.3$. Theoretical work by Smith seems to confirm this view. The g -values reported here showed considerable covalent bond character. Also, the in-plane σ -covalency parameter, $\alpha^2(Cu)$ was calculated by

$$\alpha^2(Cu) = (A_{\parallel} / 0.036) + (g_{\parallel} - 2.002) + 3 / 7g - 2.002 + 0.04 \quad (6)$$

The calculated values suggest a covalent bonding [38,56]. The in-plane and out-of-plane-bonding coefficients β_1^2 and β_2^2 respectively, are dependent upon the values of ΔE_{xy} and ΔE_{xz} in the following equations [58].

$$\alpha^2 \beta^2 = (g_{\perp} - 2.002) \Delta E_{xy} / 2_0 \quad (7)$$

$$\alpha^2 \beta_1^2 = (g_{\parallel} - 2.002) \Delta E_{xz} / 8_0 \quad (8)$$

In this work, the compounds showed β_1^2 values indicating a moderate degree of covalency in the in-plane -bonding [56,59]. However, the β^2 value for compounds indicating ionic character of the out-of-plane [60-67]. It is possible to calculate approximate orbital populations for orbitals by

$$A_{\parallel} = A_{iso} - 2B[1 \pm (7/4)\Delta g_{\parallel}](\Delta g_{\parallel} = g - g_e) \quad (9)$$

$$a_d^2 = 2B / 2B^{\circ} \quad (10)$$

Where A° and $2B^{\circ}$ is the calculated dipolar coupling for unit occupancy of d orbital respectively. When the data are analyzed, the components of the [60] Cu hyperfine coupling were considered with all the sign combinations. The only physically meaningful results are found when A_{\perp} and A_{\parallel} were negative. The resulting isotropic coupling constant was negative and the parallel component of the dipolar coupling $2B$ is negative Table 5. These results can only occur for an orbital involving the $d_{(x^2-y^2)}$ atomic orbital on copper [68-71]. The value for $2B$ is quite normal for copper(II) compounds. The A_{iso} value was relatively small. The $2B$ value divided by $2B^{\circ}$ (The calculated dipolar coupling for unit occupancy of $d_{(x^2-y^2)}$ (235.11 G), using equation (10)) suggests all orbital population are 60, 66, and 57.2% d -orbital spin density, clearly the orbital of the unpaired electron is $d_{(x^2-y^2)}$. However, Co(II) compound (6) showed isotropic spectrum with 2.12 with covalent bond character [71].

Thermal analyses (DTA and TGA)

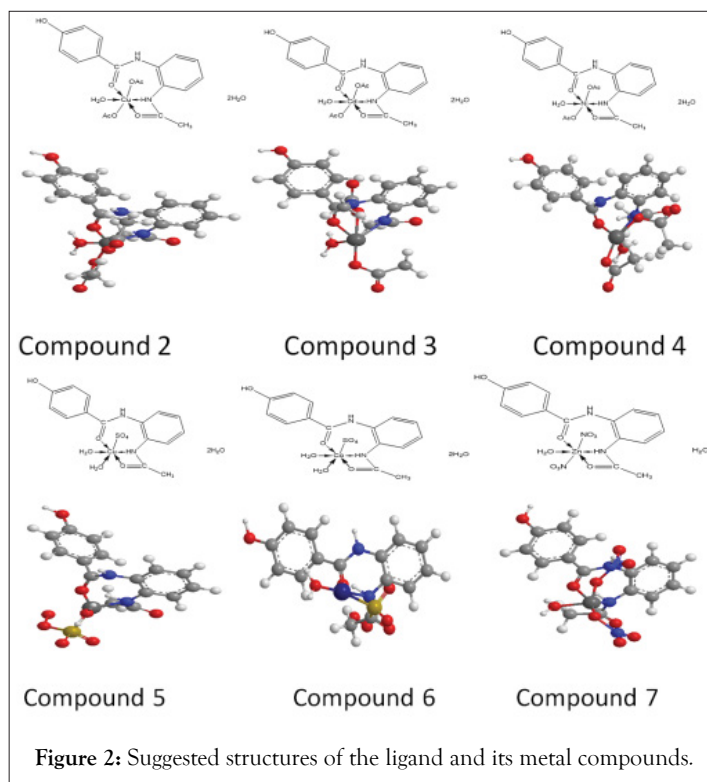
The thermal data of compounds (2), (4), (6) and (7) are listed in Table 6. These compounds were introduced as representative examples. Thermogram of compound (2) showed decomposition in six steps, the first step involving breaking of H-bondings accompanied with endothermic peak at 55°C. In the second step, two molecules of hydrated water molecules were lost endothermically with peak at 80°C accompanied by 6.1% (Calc 5.58%) weight loss. Loss of one coordinated water molecule was recorded in the third step as an endothermic peak at 145°C with 4.21 (Calc. 3.94) weight loss. The 26.52% weight loss (Calc. 26.91%) accompanied by an endothermic peak at 265°C-290°C range was assigned to loss of coordinated 2(OAc) group, whereas the endothermic peak observed at 330°C refers to the melting point of the compound. The final step observed as exothermic peaks at 445°C, 492°C, 550°C and 610°C with 23.0% weight loss (Calc. 22.15%), refers to complete decomposition of the compound which exposed up with the formation of CuO [72-78]. The first step observed in the thermogram of compound (4) involves breaking of H-bondings accompanied with endothermic peak at 58°C. In the second step, two molecules of hydrated water were lost endothermically with peak at 65 accompanied by 6.96% (Calc 7.40%) weight loss. In

Table 5: The ESR data for metal (II) compounds.

Complex	g_{\parallel}	g_{\perp}	g_{iso}	A_{\parallel} (G)	A_{\perp} (G)	A_{iso} (G)	$^{\circ}G$	ΔE_{xy} (cm ⁻¹)	ΔE_{xz} (cm ⁻¹)	K^2_{\perp}	K^2_{\parallel}	K^2	K	$g_{\parallel}/A_{\parallel}$ (cm ⁻¹)	α^2	β^2	β_1^2	-2β	a^2d (%)
2	2.18	2.06	2.13	135	7.5	50	3.00	17241	21052	0.73	0.46	1.01	0.8	155.7	0.63	1.16	0.73	141	60
5	2.19	2.07	2.11	120	15	30	2.7	17391	21739	0.89	0.49	0.76	0.87	182.5	0.59	1.51	0.83	134	57.2
6	-	-	2.12	-	-	-	-	-	-	-	-	-	-	-	-	-	-	-	-

Table 6: Thermal analyses for some metal (II) compounds.

Compound no. molecular formula	Temp. (°C)	DTA (peak)		TGA (Wt.loss %)		Assignments
		Endo	Exo	Calc	Found	
Compound 2	55	endo	-	-	-	Broken of H-bondings
	80	endo	-	5.58	6.1	Loss of (2H ₂ O) hydrated water molecules
	145	endo	-	3.94	4.21	Loss of (H ₂ O) coordinated water molecule
	265,290	endo	-	26.91	26.52	Loss of coordinated 2(OAc) group
	330	endo	-	-	-	Melting point
Compound 3	445,492,550,610	-	Exo	22.15	23	Decomposition process with the formation of (CuO)
	58	endo	-	-	-	Broken of H-bondings
	65	endo	-	7.4	6.96	Loss of (2H ₂ O) hydrated water molecule
	160	endo	-	7.34	7.1	Loss of (2H ₂ O) coordinated water molecules
	285,300	endo	-	18.52	18.63	Loss of coordinated 2(OAc) group
Compound 6	330	endo	-	-	-	Melting point
	470,515,580	-	Exo	26.5	26.81	Decomposition process with the formation of (NiO)
	52	endo	-	-	-	Broken of H-bondings
	80	endo	-	4.31	4.1	Loss of (2H ₂ O) hydrated water molecule
	120	endo	-	5.21	5.62	Loss of (H ₂ O) coordinated water molecule
Compound 7	265,282	endo	-	30.9	31.22	Loss of coordinated SO ₄ group
	330	endo	-	-	-	Melting point
	425,480,530,600	-	Exo	30.7	31.4	Decomposition process with the formation of (CoO)
	55	endo	-	-	-	Broken of H-bondings
	80	endo	-	5.58	6.1	Loss of (H ₂ O) hydrated water molecule
Compound 4	145	endo	-	3.94	4.21	Loss of (H ₂ O) coordinated water molecule
	265,290	endo	-	26.91	26.52	Loss of coordinated 2(NO ₂) group
	330	endo	-	-	-	Melting point
	445,492,550,610	-	Exo	18.5	19.2	Decomposition process with the formation of (ZnO)



the third step, two molecules of coordinated water molecules were lost endothermically with a peak at 160°C accompanied by 7.10% (Calc. 7.34%) weight loss. The fourth step involved loss of coordinated 2(OAc) group accompanied with an endothermic peak at 285°C-300°C range with 18.63% (Calc. 18.52%). while the

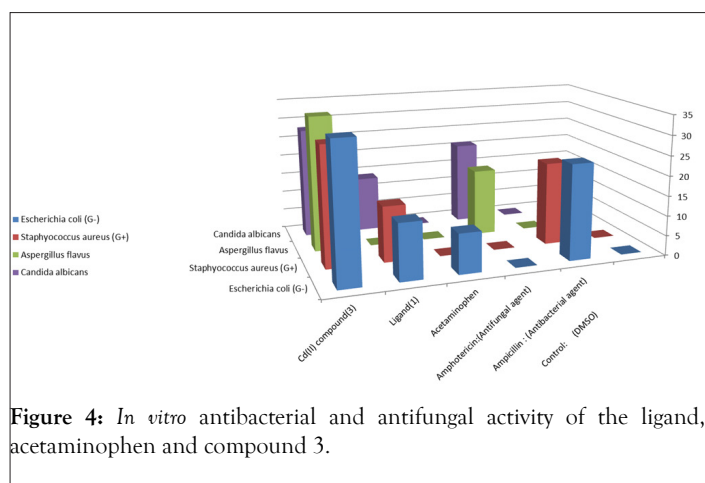
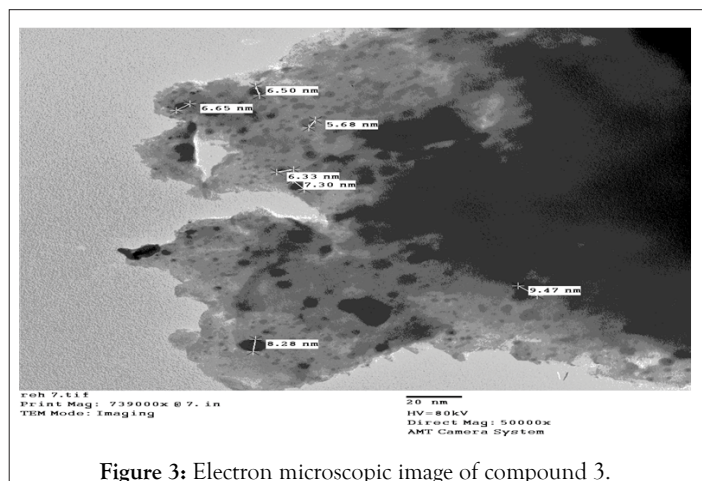




Figure 5: *In vitro* antibacterial and antifungal activity of the ligand and acetaminophen.

endothermic peak appeared at 330°C refers to the melting point of the compound. The final step observed at 470°C, 515°C and 580°C with 26.81% weight loss (Calc. 26.50%) as exothermic peaks, refers to complete oxidative decomposition of the compound which ended up with the formation of NiO. The first step observed in the thermogram of compound (6) involving breaking of H-bondings accompanied with endothermic peak at 48°C. In the second step, two molecules of hydrated water were lost endothermically with peak at 80°C accompanied by 4.1% (Calc. 4.31%) weight loss. Loss of one coordinated water molecule was recorded in the third step as an endothermic peak at 120°C with 5.62 (Calc. 5.21%) weight losses. The 31.22% weight loss (Calc. 30.9%) accompanied by an endothermic peak appears at 265°C-282°C was assigned to loss of coordinated SO₄ group whereas the endothermic peak observed at 330°C refers to the melting point of the compound. The final step observed at 425°C, 480°C, 530°C and 600°C with 31.4% weight loss (Calc. 30.7%), refers to complete oxidative decomposition of the compound which exposed up with the formation of CoO. The first step observed in the thermogram of compound (7) involving breaking of H-bondings accompanied with endothermic peak at 55°C. In the second step, one molecule of hydrated water was lost endothermically with peak at 80°C accompanied by 6.1% (Calc. 5.58%) weight loss. The third step involved loss of one coordinated water molecule accompanied with an endothermic peak at 145°C with 4.21 (Calc. 3.94%). The 26.52% weight loss (Calc. 26.91%) accompanied by an endothermic peak appears at 265°C-290°C range was assigned to loss of coordinated 2(NO₃) group, whereas the endothermic peak observed at 330°C refers to the melting point of the compound. The final step observed at 445°C, 492°C, 550°C and 610°C with 19.2% weight loss (Calc. 18.50%), refers to complete oxidative decomposition of the compound which exposed up with the formation of ZnO.

Antimicrobial activity

In vitro biological screening tests of the ligand (1) and its metal compounds (2), (3), (4), (5), (6) and (7) carried out as antibacterial and antifungal activity (Figures 4-8). The antibacterial activity was tested against two bacterial strains; Gram-positive *Staphylococcus aureus* as well as Gram-negative *Escherichia coli* strains [79,80]. The results compared with standard drugs (Ampicillin (Gram positive) and (Gram negative) as a standard drug. The compounds were also subjected to antifungal activity against *Aspergillus flavus* and *Candida albicans* using Amphotericin B as a standard drug [81-83]. The data indicated that, using low concentration against microbes, acetaminophen and ligand no effect was observed. However, the compounds show moderate to high effect, the order for Gram positive is (3)>(6)>standard>(4)>(5)>(2)>(7)>acetaminophen=ligand and Gram negative was (3)> standard>(6)>(4)>(5)>(2)>(7)>acetaminophen=ligand and *Aspergillus flavus* was (3)>standard> acetaminophen=ligand=(2)=(4)=(5)=(6)=(7) and *Candida albicans* is (3)>standard>(4)>(6)>(5)>(2)> acetaminophen=ligand=(7). In case of high concentration, the order of activity for Gram positive was (3)>standard>ligand>acetaminophen and for Gram negative (3)>standard>ligand>acetaminophen and for *Aspergillus flavus* was



Figure 6: *In vitro* antibacterial and antifungal activity of compound 3.

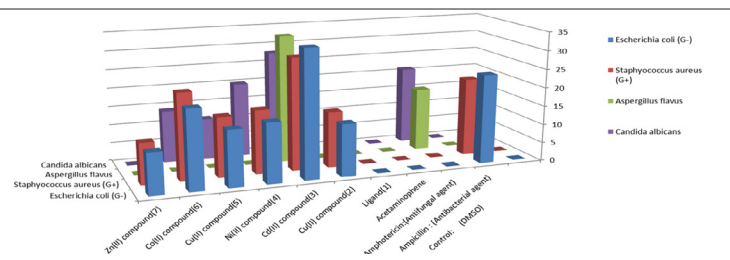


Figure 7: *In vitro* antibacterial and antifungal activity of some metal compounds.



Figure 8: *In vitro* antibacterial and antifungal activity of some metal compounds.

(3)>standard>ligand=acetaminophen and for *Candida albicans* was (3)>standard>ligand>acetaminophen. *In vivo* studies showed no side effect was observed for all organs tested. The major groups of antibiotics that are currently in use have three microbial targets: the cell wall synthesis, translational machinery and DNA replication machinery. Unfortunately, microbial resistance can developed against each of these modes of action. Most of the antibiotic resistance mechanisms are irrelevant for nanoparticles (NPs) because the mode of action of NPs is direct contact with the microbial cell wall without the need to penetrate the cell. This raises the hope that NPs would be less prone to promote resistance in microbes than antibiotics. Most microbes exist in the form of a biofilm which often contains diverse species that interact with each other and their environment. Biofilms are specifically microbial aggregates that rely on a solid surface and extracellular products, such as extracellular polymeric substances (EPSs). Microbes move reversibly onto the surface but the expression of EPSs renders the attachment irreversible. Once the microbes settled, synthesis of the microbial flagellum is inhibited and the microbes multiply rapidly resulting in the development of a mature biofilm. At this stage, the microbes are stuck together, forming a barrier that can resist antibiotics and provide a source of systemic chronic infections, thus, biofilm are a serious health threat. Nano materials are materials that have at least one dimension (1-100 nm) in the nanometer scale. NPs have demonstrated broad-spectrum antimicrobial properties. The antimicrobial mechanism of action of NPs is generally described as adhering to one of three models: oxidative stress induction, metal ion release, or non-oxidative mechanism [84-89]. These three types of mechanisms can occur simultaneously [89-91]. Nano Cd(II) compound (3) showed higher activity compared with the standard and other compounds. It may be Cd(II) compound prompt neutralization of the surface electric charge of the microbial membrane and change its penetrability, ultimately leading to microbial death [92-94]. *In vitro* antibacterial

and antifungal activity of the ligand, acetaminophen and compound(3) and also other compounds are shown in Tables 7 and 8.

Transmission electron microscopy characterization (TEM)

TEM images for the colloidal suspensions of Cd(II) compound was obtained. The average diameter of these spherical Cd compound was found to be 7.17 ± 1.30 nm as shown in Figure 9.

As shown, the compound is present in nano size particles i.e., its particles present in a diameter between 1 nanometer and 100 nanometers in size [95-100]. Nanoparticles can be defined as particles less than 100 nm in diameter that exhibit new or enhanced size-dependent properties compared with larger particles of the same material with many advantages such as:

1. Increased bioavailability

2. Dose proportionality
3. Decreased toxicity
4. Smaller dosage form (i.e., smaller tablet)
5. Stable dosage forms of drugs which are either unstable or have unacceptably low bioavailability in non-nanoparticulate dosage forms.
6. Increased active agent surface area results in a faster dissolution of the active agent in an aqueous environment, such as the human body.
7. Faster dissolution generally equates with greater bioavailability, smaller drug doses, less toxicity.
8. Reduction in fed/fasted variability.

Table 7: *In vitro* antibacterial and antifungal activity of the ligand, acetaminophen and compound 3.

	<i>Escherichia coli</i> (G-)	<i>Staphyococcus aureus</i> (G+)	<i>Aspergillus flavus</i>	<i>Candida albicans</i>
Control: (DMSO)	0	0	0	0
Ampicillin : (Antibacterial agent)	24	21	0	0
Amphotericin: (Antifungal agent)	0	0	17	21
Acetaminophen	10	0	0	0
Ligand 1	14	14	0	14
Cd(II) compound 3	34	30	34	28

Table 8: *In vitro* antibacterial and antifungal activity of some nano-metal compounds.

	<i>Escherichia coli</i> (G-)	<i>Staphyococcus aureus</i> (G+)	<i>Aspergillus flavus</i>	<i>Candida albicans</i>
Control: (DMSO)	0	0	0	0
Ampicillin : (Antibacterial agent)	24	21	0	0
Amphotericin:(Antifungal agent)	0	0	17	21
Acetaminophene	0	0	0	0
Ligand(1)	0	0	0	0
Cu(II) compound 2	14	15	0	10
Cd(II) compound 3	34	30	34	28
Ni(II) compound 4	16	17	0	20
Cu(II) compound 5	15	16	0	11
Co(II) compound 6	21	23	0	14
Zn(II) compound 7	11	11	0	0

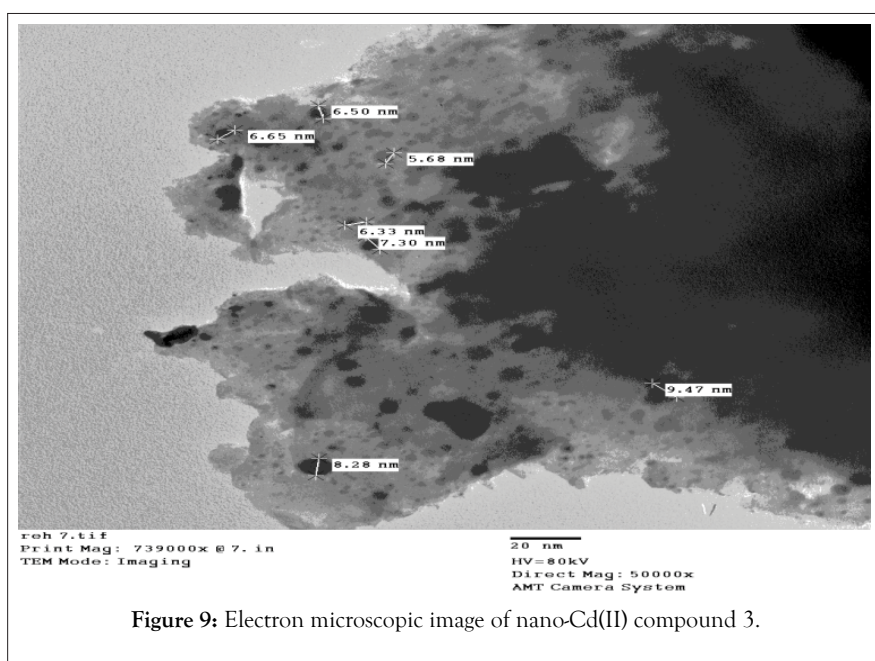


Figure 9: Electron microscopic image of nano-Cd(II) compound 3.

In vivo toxicity studies

Determination of liver functions AST, ALT, and albumin in the serum of normal rats show no significant differences between treated groups and the control group (Tables 9 and 10, Figures 10 and 11).

Haematological studies

There are no any significant differences in renal functions or hematological parameters between all tested groups (Table 11, Figure 12) [101].

Figure 13 shows the Development stages of medicine.

Antivirus activity

The great majority has an RNA genome, which is usually small and single strand (SS), but some viruses have double stranded (ds) RNA, SS DNA or ds DNA genomes. Transmission of a virus by insects is a specific biological process. The photographs of the plant before and after treatment are in Figures 14 and 15.

CONCLUSION

Most plant viruses are rod-shaped with protein discs forming a tube surrounding the viral genome, isometric particles are another common structure. They rarely have an envelope. The great majority have an RNA genome, which is usually small and Single

Table 9: Statistical analysis (ANOVA) for liver function tests in the different groups treated with Cd(II) compound 3 NPs.

Parameters	Control	Cd NPs (1×10^5 mmole/L)	Cd NPs (2×10^5 mmole/L)
AST (U/l)	50.20 \pm 3.66 ^{ac}	48.35 \pm 4.34 ^b	51.36 \pm 3.22 ^{ac}
ALT (U/l)	36.9 \pm 4.81 ^a	27.90 \pm 6.91 ^{bc}	26.750 \pm 2.14 ^{bc}
Alb (g/dl)	3.90 \pm 1.12 ^a	4.20 \pm 1.71 ^{bc}	4.170 \pm 1.55 ^{bc}

ANOVA: Analysis of Variance; AST: Aspartate aminotransferase; ALT: Alanine aminotransferase; Alb: Albumin; SD: Standard Deviation. Each value is represented as mean \pm SD. Data with different superscripts are significantly different at $p \leq 0.05$.

Note: ^aSignificance versus control group; ^bSignificance versus group treated with Cd NPs with 1×10^5 mmole/L; ^cSignificance versus group treated with Cd NPs with 2×10^5 mmole/L.

Table 10: Statistical analysis (ANOVA) for renal function tests in the different groups treated with Cd(II) compound 3 NPs.

Parameters	Control	Cd NPs (1×10^5 mmole/L)	Cd NPs (2×10^5 mmole/L)
B. Urea (mg/dl)	33.40 \pm 2.79 ^a	36.10 \pm 3.55 ^{bc}	35.40 \pm 2.89 ^{bc}
S. Creatinine (mg/dl)	0.52 \pm 0.11 ^{ab}	0.51 \pm 0.17 ^{ab}	0.565 \pm 0.971 ^c

ANOVA: Analysis of Variance; SD: Standard Deviation. Each value is represented as mean \pm SD. Data with different superscripts are significantly different at $p \leq 0.05$.

Note: ^aSignificance versus control group; ^bSignificance versus group treated with Cd(II) compound 3 NPs with 1×10^5 mmole/L; ^cSignificance versus group treated with Cd(II) compound 3 NPs with 2×10^5 mmole/L.

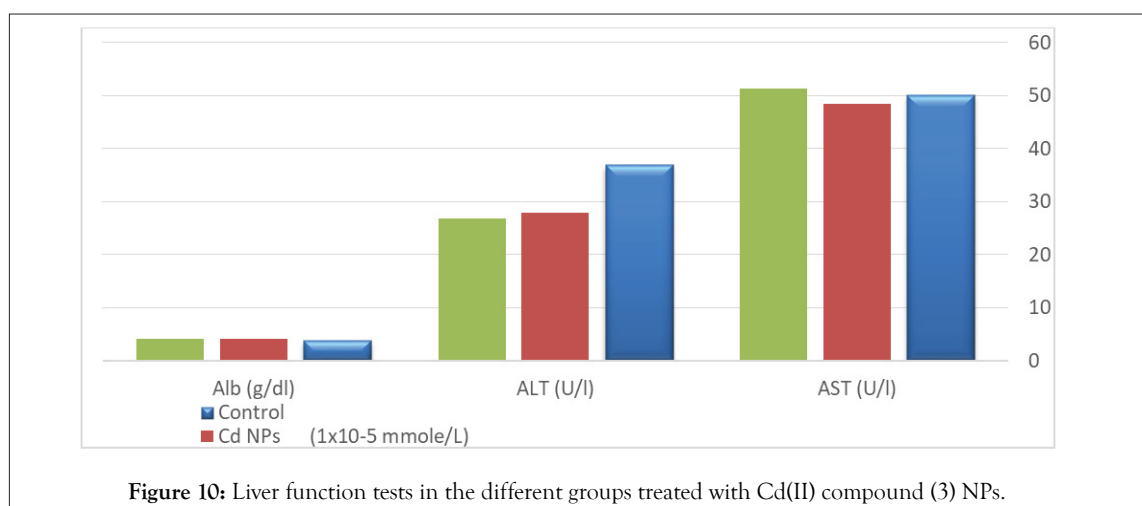


Figure 10: Liver function tests in the different groups treated with Cd(II) compound (3) NPs.

Table 11: Statistical analysis (ANOVA) for hematological tests in the different groups treated by Cd(II) compound 3 NPs.

Parameters	Control	Cd NPs (6 Weeks)	Cd NPs (12 Weeks)
Hb (g/dl)	15.70 \pm 2.16 ^{ab}	15.80 \pm 2.89 ^{ab}	16.20 \pm 1.980 ^c
RBCs ($\times 10^6$ /cmm)	6.11 \pm 0.71 ^{abc}	6.52 \pm 1.12 ^{abc}	6.71 \pm 1.760 ^{abc}
TLC ($\times 10^3$ /cmm)	9.90 \pm 2.14 ^{ac}	10.80 \pm 1.77 ^b	10.10 \pm 1.680 ^{ac}
PLTs ($\times 10^3$ /cmm)	414.42 \pm 18.92 ^{ac}	448.30 \pm 26.41 ^b	398.81 \pm 22.17 ^{ac}

ANOVA: Analysis of Variance; Hb: Hemoglobin concentration; RBCs: Red Blood Corpuscles count; T.L.C: Total Leucocytic Count; PLT: Platelets count. Each value is represented as mean \pm SD. Data with different superscripts are significantly different at $p \leq 0.05$.

Note: ^aSignificance versus control group; ^bSignificance versus group treated with Cd(II) compound 3 NPs with 1×10^5 mmole/L; ^cSignificance versus group treated with Cd(II) compound 3 NPs with 2×10^5 mmole/L.

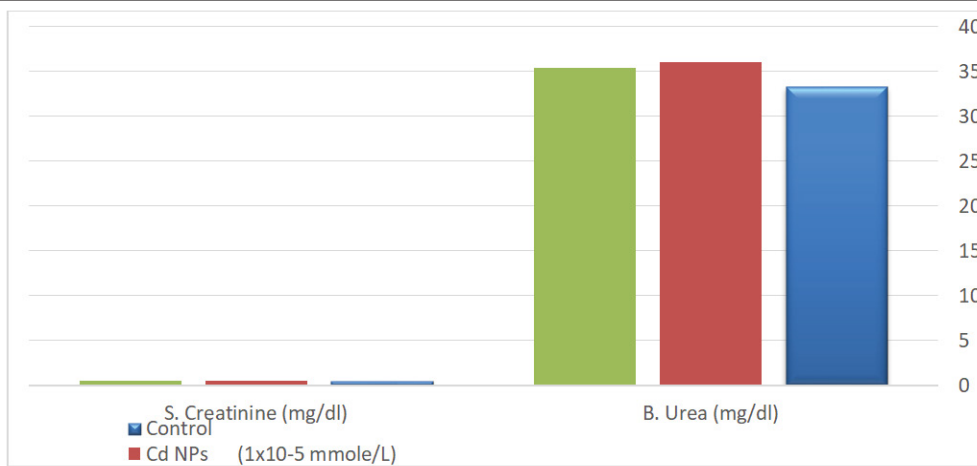


Figure 11: Renal function tests in the different groups treated with Cd(II) compound 3 NPs.

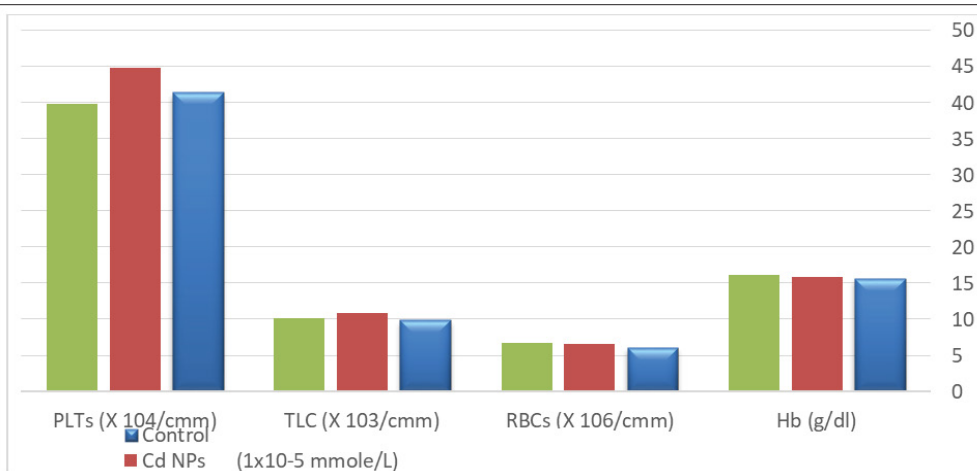


Figure 12: Hematological tests in the different groups treated by Cd(II) compound 3 NPs.



Figure 13: Development stages of medicine.



Figure 14: Plant before spraying.



Figure 15: Plant after spraying.

Strand (SS), but some viruses have double stranded (ds) RNA, SS DNA or ds DNA genomes. Transmission of a virus by insects is a specific biological process. The majority of aphids-transmitted viruses affecting plants are transmitted in a non-persistent way. Use Cd(II) nano compound spray to deter aphids from landing and feeding. This method delay virus infection rather than totally prevent it. Spray is very effective in killing aphids breeding on plants and can provide good control of viruses transmitted in a

persistent manner. After one week of sprayed the infected plant with Cd(II) nano compound, improvement in leaf surface was observed and growth of the plant was occurred.

Due to the difficulty of testing the nano-Cd(II) compound (3) on animal viruses in our labs, we applied it on plant viruses and impressive results were obtained as shown in plant photographs and this gives us hope for applying it on animal viruses, for example corona virus.

ACKNOWLEDGEMENTS

This study was supported by Taif University Researches supporting project number (TURSP-2020/157) Taif University, Taif, Saudi Arabia.

REFERENCES

- Matelaa G, Amana R, Sharmab C, Chaudharyc S. Synthesis, characterization and antimicrobial evaluation of diorganotin (IV) complexes of schiff base. *Indian J Adv Chem Sci.* 2013; 1(3):157-163.
- Abdou S. El-Tabl, Moshira M. Abd El-Wahed and Salah. M. Khalefa, Synthesis and spectroscopic characterization of bioactive compounds derived from glutamic acid; study of their antimicrobial and antiproliferative properties, *International Journal of Scientific and Engineering Research*, 2018, Vol.9(2),p 2114-2126.
- Correia I, Adao P, Roy S, Wahba M, Matos C, Maurya MR, et al. Hydroxyquinoline derived vanadium (IV and V) and copper (II) complexes as potential anti-tuberculosis and anti-tumor agents. *J Inorg Biochem.* 2014; 141:83-93.
- Kondaiah S, Reddy GN, Rajesh D, Joseph J. Synthesis, characterization, and antibacterial activity of the schiff base derived from P-toluic hydrazide and O-vanilin (OVPTH Ligand) and its Mn (II), Co (II), Ni (II) and Cu (II) complexes. *Indian J Adv Chem Sci.* 2013; 1(4):228-235.
- Abdou S, Shakdofa MM, Whaba MA. Synthesis, characterization and fungicidal activity of binary and ternary metal (II) complexes derived from 4, 4'-(4-nitro-1, 2-phenylene) bis (azanylylidene)) bis (3-(hydroxyimino) pentan-2-one). *Spectrochim Acta A.* 2015; 136:1941-1949.
- El-Bahnasawy RM, El-Saied FA, Gaafer EH, Wahba MA. Benzil bisisonicotinoyl hydrazone complexes of trivalent metals Ti, Zr, Sn, Hf and Th. *Inorg Chem Indian J.* 2013; 8:1-6.
- El-Tabl A, Wahed MAE, Wahba MA. Spectroscopic characterization and cytotoxic activity of new metal complexes derived from (1E, N'Z, N'Z)-N',N'-bis(2-hydroxybenzylidene)-2-(naphthalen-1-lyoxy) acetohydrazonehydrazide. *JAC.* 2015; 11: 3888-3918.
- El-Tabl AS, Wahed MMAE, Wahba MA, El-assaly SA, Saad LM. Sugar hydrazone complexes; Synthesis, spectroscopic characterization and antitumor activity. *JAC.* 2014; 9: 1837-1860.
- Bacchi A, Carcelli M, Pelagatti P, Pelizzi G, Rodriguez-Arguelles M, Rogolino D, et al. Antimicrobial and mutagenic properties of organotin (IV) complexes with isatin and N-alkylisatin bisthiocarbonohydrazones. *J Inorg Biochem.* 2005; 99: 397-408.
- Bacchi A, Bonardi A, Carcelli M, Mazza P, Pelagatti P, Pelizzi C, et al. Organotin complexes with pyrrole-2, 5-dicarboxaldehyde bis (acylhydrazones). Synthesis, structure, antimicrobial activity and genotoxicity. *J Inorg Biochem.* 1998; 69(1-2):101-112.
- El-Asmy AA, El-Gammal OA, Radwan HA. Synthesis, characterization and biological study on Cr 3+, ZrO 2+, HfO 2+ and UO2 2+ complexes of oxalohydrazide and bis (3-hydroxyimino) butan- 2-ylidene)-oxalohydrazide. *Spectrochim Acta A Mol Biomol Spectrosc.* 2010; 76(5): 496-501.
- El-Asmy AA, El-Gammal OA, Radwan HA, Ghazy SE. Ligational, analytical and biological applications on oxalyl bis (3, 4-dihydroxybenzylidene) hydrazone. *Spectrochim Acta A Mol Biomol Spectrosc.* 2010; 77(1):297-303.
- Machakanur SS, Patil BR, Badiger DS, Bakale RP, Gudasi KB, Bligh SA. Synthesis, characterization and anticancer evaluation of novel tri-arm star shaped 1, 3, 5-triazine hydrazones. *J Mol Struct.* 2012; 1011:121-127.
- El-Asmy AA, Al-Abdeen AZ, El-Maaty WA, Mostafa MM. Synthesis and spectroscopic studies of 2, 5-hexanedione bis (isonicotinylhydrazone) and its first raw transition metal complexes. *Spectrochim Acta A Mol Biomol Spectrosc.* 2010; 75(5):1516-1522.
- Svehla G. *Textbook of Macro and Semimicro Qualitative Inorganic Analysis.* Vogel's, Library of Congress Cataloging in Publication Data, New York. 1985.
- Yoe JH. The analytical uses of ethylenediaminetetraacetic acid. *J Am Chem Soc.* 1958; 80(10):2600.
- El-Tabl AS, Mohamed Abd El-Waheed M, Wahba MA, Abou El-Fadl AE. Synthesis, characterization, and anticancer activity of new metal complexes derived from 2-hydroxy-3-(hydroxyimino)-4-oxopentan-2-ylidene) benzohydrazide. *Bioinorg Chem Appl.* 2015; 2015.
- Narang KK, Singh VP. Synthesis and characterization of cobalt(II), nickel(II), copper(II) and zinc (II) complexes with acetylacetone bis-benzoylhydrazone and acetylacetone bis- isonicotinoylhydrazone, *Transit Met Chem.* 1993; 18:287-290.
- Rouzer CA. Metals and DNA repair. *Chem Res Toxicol.* 2010; 23(3):1517-1518.
- Vandavelde NM, Tulkens PM, Van Bambeke F. Modulating antibiotic activity towards respiratory bacterial pathogens by co-medications: a multi-target approach. *Drug Discov Today* 2016; 21(7):1114-1129.
- Khan I, Saeed K, Khan I. Nanoparticles: Properties, applications and toxicities. *Arab J Chem.* 2019; 12(7):908-931.
- Vogel AI. *A Text Book of Quantitative Inorganic Analysis.* 1978; 609.
- Figgis BN, Lewis J, Wilkins RG. *Modern coordination chemistry.* New York: Interscience. 1960.
- Vichai V, Kirtikara K. Sulforhodamine B colorimetric assay for cytotoxicity screening. *Nat Protoc.* 2006; 1(3):1112-1116.
- Nagesh GY, Mruthyunjayaswamy BH. Synthesis, characterization and biological relevance of some metal (II) complexes with oxygen, nitrogen and oxygen (ONO) donor Schiff base ligand derived from thiazole and 2-hydroxy-1-naphthaldehyde. *J Mol Struct.* 2015; 1085:198-206.
- Geary WJ. The use of conductivity measurements in organic solvents for the characterisation of coordination compounds. *Coord Chem Rev.* 1971; 7(1):81-122.
- Pouralimardan O, Chamayou AC, Janiak C, Hosseini-Monfared H. Hydrazone Schiff base-manganese(II) complexes: Synthesis, crystal structure and catalytic reactivity. *Inorganica Chim Acta.* 2007; 360(5):1599-608.
- Gup R, Kirkan B. Synthesis and spectroscopic studies of copper (II) and nickel (II) complexes containing hydrazonic ligands and heterocyclic coligand. *Spectrochim Acta A Mol Biomol Spectrosc.* 2005; 62(4-5):1188-1195.
- Babu SV, Reddy KH. Second derivative spectrophotometric determination of copper (II) using 2-acetylpyridine semicarbazone in biological, leafy vegetable and synthetic alloy samples. *Indian J Adv Chem Sci.* 2013; 1(2):105-111.
- Hosseini-Monfared H, Asghari-Lalami N, Pazio A, Wozniak K, Janiak C. Dinuclear vanadium, copper, manganese and titanium complexes containing O, O, N-dichelating ligands: Synthesis, crystal structure and catalytic activity. *Inorganica Chim Acta.* 2013; 406:241-250.
- Chanu OB, Kumar A, Ahmed A, Lal RA. Synthesis and characterisation of heterometallic trinuclear copper (II) and zinc (II) complexes derived from bis (2-hydroxy-1-naphthaldehyde) oxaloyldihydrazone. *J Mol Struct.* 2012; 1007:257-274.
- Kar NK, Singh MK, Lal RA. Synthesis and spectral studies on heterobimetallic complexes of manganese and ruthenium derived from bis [N-(2-hydroxynaphthalen-1-yl) methylene] oxaloyldihydrazone. *Arab J Chem.* 2012; 5(1):67-72.
- Fouda MF, Abd-Elzaher MM, Shakdofa MM, El-Saied FA, Ayad MI,

- El Tabl AS. Synthesis and characterization of a hydrazone ligand containing antipyrine and its transition metal complexes. *J Coord Chem*. 2008; 61(12):1983-1996.
34. Fouda MF, Abd-Elzاهر MM, Shakhdoفا MM, El Saied FA, Ayad MI, El Tabl AS. Synthesis and characterization of transition metal complexes of N'-(1, 5-dimethyl-3-oxo-2-phenyl-2, 3-dihydro-1H-pyrazol-4-yl) methylene] thiophene-2-carbohydraزide. *Transit Met Chem*. 2008; 33(2):219-228.
 35. Gudasi KB, Patil MS, Vadavi RS, Shenoy RV, Patil SA, Nethaji M. X-ray crystal structure of the N-(2-hydroxy-1-naphthalidene) phenylglycine Schiff base. Synthesis and characterization of its transition metal complexes. *Transit Met Chem*. 2006; 31(5):580-585.
 36. Maurya MR, Khurana S, Schulzke C, Rehder D. Dioxo-and Oxovanadium (V) Complexes of Biomimetic Hydrazone ONO Donor Ligands: Synthesis, Characterisation, and Reactivity. *Eur J Inorg*. 2001; 2001(3):779-788.
 37. Tossidis IA, Bolos CA. Monohalogenobenzoylhydrazones II. Synthesis and study of Ti (IV) complexes with monochlorobenzoylhydrazones of 2-furaldehyde, 2-thiophenaldehyde, 2-pyrrolaldehyde and di-2-pyridylketone as ligands. *Inorganica chim acta*. 1986; 112(1):93-97.
 38. Hong M, Yin H, Zhang X, Li C, Yue C, Cheng S. Di- and tri-organotin (IV) complexes with 2-hydroxy-1-naphthaldehyde 5-chloro-2-hydroxybenzoylhydrazone: Synthesis, characterization and *in vitro* antitumor activities. *J Organomet Chem*. 2013; 724:23-31.
 39. Maurya MR, Agarwal S, Bader C, Rehder D. Dioxovanadium (V) Complexes of ONO Donor Ligands Derived from Pyridoxal and Hydrazides: Models of Vanadate-Dependent Haloperoxidases. *Eur J Inorg*. 2005; 2005(1):147-157.
 40. Abd El-Wahab ZH, Mashaly MM, Salman AA, El-Shetary BA, Faheim AA. Co (II), Ce (III) and UO₂ (VI) bis-salicylatothiosemicarbazide complexes: binary and ternary complexes, thermal studies and antimicrobial activity. *Spectrochim Acta A Mol Biomol Spectrosc*. 2004; 60(12):2861-2873.
 41. Nakamoto K. *Infrared and Raman Spectra of Inorganic and Coordination Compounds*. Wiley Online Library. 1986.
 42. Gupta LK, Bansal U, Chandra S. Spectroscopic and physicochemical studies on nickel (II) complexes of isatin-3, 2'-quinolyl-hydrazones and their adducts. *Spectrochim Acta A Mol Biomol Spectrosc*. 2007; 66(4-5):972-975.
 43. El-Tabl AS, Shakhdoفا MM, Shakhdoفا AM. Metal complexes of N'-(2-hydroxy-5-phenyldiazanyl) benzylideneisonicotinohydraزide: Synthesis, spectroscopic characterization and antimicrobial activity. *J Serb Chem*. 2013; 78(1):39-55.
 44. El-Tabl AS, Shakhdoفا MM, El-Seidy AM, Al-Hakimi AN. Synthesis, characterization and antifungal activity of metal complexes of 2-(5-((2-chlorophenyl) diazenyl)-2-hydroxybenzylidene) hydrazinecarbothioamide. *Phosphorus Sulfur Silicon Relat Elem*. 2012; 187(11):1312-1323.
 45. Chandra S, Gupta LK. Spectroscopic studies on Co (II), Ni (II) and Cu (II) complexes with a new macrocyclic ligand: 2, 9-dipropyl-3, 10-dimethyl-1, 4, 8, 11-tetraaza-5, 7: 12, 14-dibenzocyclotetradeca-1, 3, 8, 10-tetraene. *Spectrochim Acta A Mol Biomol Spectrosc*. 2005; 61(6):1181-1188.
 46. El Saied FA, Shakhdoفا MM, El Tabl AS, Abd Elzاهر MM. Coordination behaviour of N' 1, N' 4-bis ((1, 5-dimethyl-3-oxo-2-phenyl-2, 3-dihydro-1H-pyrazol-4-yl) methylene) succinohydraزide toward transition metal ions and their antimicrobial activities. *Main Group Chem*. 2014; 13(2):87-103.
 47. El-Tabl AS. Synthesis, characterisation and antimicrobial activity of manganese (II), nickel (II), cobalt (II), copper (II) and zinc (II) complexes of a binucleating tetradentate ligand. *J Chem Res*. 2002; 2002(11):529-531.
 48. Aly MM, Imam SM. Characterization of Copper (II), nickel (II), cobalt (II) and palladium (II) complexes of vicinal oxime-imine ligands; induced chelate isomerism in the same molecule of the nickel (II) complex. *Monatsh Chem*. 1995; 126(2):173-185.
 49. Lever ABP. *Inorganic Electronic Spectroscopy*, Amsterdam, Elsevier. 1968.
 50. Xiang GQ, Zhang LX, Zhang AJ, Cai XQ, Hu ML. 6-(2, 4-Difluorophenyl)-3-(3-methylphenyl)-7H-1, 2,4-triazolo[3, 4-b] [1, 3, 4] thiadiazine. *Acta Crystallogr Sect E: Struct Rep Online*. 2004; 60(12): 02249-02251.
 51. Parihari RK, Patel RK, Patel RN. Synthesis and characterization of metal complexes of manganese, cobalt and zinc (II) with Schiff base and some neutral ligand. *J Indian Chem Soc*. 2000; 77(7):339-40.
 52. Goel S, Chandra S, Dwivedi SD. Synthesis, spectral and biological studies of copper (II) and iron (III) complexes derived from 2-acetyl benzofuran semicarbazone and 2-acetyl benzofuran thiosemicarbazone. *J Saudi Chem Soc*. 2016; 20(6):651-660.
 53. El-wakiel N, El-Keiy M, Gaber M. Synthesis, spectral, antitumor, antioxidant and antimicrobial studies on Cu (II), Ni (II) and Co (II) complexes of 4-[(1H-Benzoimidazol-2-ylimino)-methyl]-benzene-1, 3-diol. *Spectrochim Acta A*. 2015; 147:117-123.
 54. Krushna C, Mohapatra C, Dash KC. 4-, 5- and 6-coordinate complexes of copper (II) with substituted imidazoles. *J Inorg Nucl Chem*. 1977; 39(7):1253-1258.
 55. Thakkar NV, Bootwala SZ. Synthesis and characterization of binuclear metal complexes derived from some isonitrosoacetophenones and benzidine. *Indian J Chem*. 1995; 34:370-374.
 56. El-Tabl AS, El-Enein SA. Reactivity of the new potentially binucleating ligand, 2-(acetichydraزido-N-methylidene- α -naphthol)-benzothiazol, towards manganese (II), nickel (II), cobalt (II), copper (II) and zinc (II) salts. *J Coord Chem*. 2004; 57(4):281-294.
 57. Abdou S, Shakhdoفا MM, Whaba MA. Synthesis, characterization and fungicidal activity of binary and ternary metal (II) complexes derived from 4, 4'-(4-nitro-1, 2-phenylene) bis (azanylylidene)) bis (3-(hydroxyimino) pentan-2-one). *Spectrochim Acta A*. 2015; 136:1941-1949.
 58. Mehta JV, Gajera SB, Patel MN. Antimalarial, antimicrobial, cytotoxic, DNA interaction and SOD like activities of tetrahedral copper (II) complexes. *Spectrochim Acta A*. 2015; 136:1881-1892.
 59. Sarkar B, Bocelli G, Cantoni A, Ghosh A. Copper (II) complexes of symmetrical and unsymmetrical tetradentate Schiff base ligands incorporating 1-benzoylacetone: Synthesis, crystal structures and electrochemical behavior. *Polyhedron*. 2008; 27(2):693-700.
 60. El-Tabl HM, El-Saied FA, Ayad MI. Manganese (II), iron (III), cobalt (II), nickel (II), copper (II), zinc (II), and uranyl (VI) complexes of n-(2-furylylidene) benzothiazol-2-ylacet ohydraزide. *Synth React Inorg Met Org Chem*. 2002; 32(7):1189-1203.
 61. Chandra S, Gupta LK, Jain D. Spectroscopic studies on Mn (II), Co (II), Ni (II), and Cu (II) complexes with N-donor tetradentate (N₄) macrocyclic ligand derived from ethylcinnamate moiety. *Spectrochim Acta A*. 2004; 60(10):2411-2417.
 62. El-Tabl AS. Synthesis and characterization of cobalt (II)/(III), nickel (II) and copper (II) complexes of new 14, 15 and 16-membered macrocyclic ligands. *B Korean Chem Soc*, 2004; 25: 1757-1763.
 63. El-Tabl AS, Shakhdoفا MM, El-Seidy A, Al-Hakimi AN. Synthesis, Characterization and Biological Studies of New Mn (II), Ni (II), Co (II), Cu (II) and Zn (II) of 2-(benzothiazol-2-yl)-N'-(2, 5-dihydroxybenzylidene) acetohydraزide. *J Korean Chem Soc*. 2011; 55(1):19-27.

64. El-Boraei HA, El-Tabl AS. Supramolecular copper (II) complexes with tetradentate ketoenamine ligands. *Pol J Chem.* 2003; 77: 1759-1775.
65. Kivelson D, Neiman R. ESR studies on the bonding in copper complexes. *J Chem Phys.* 1961; 35(1):149-155.
66. Procter IM, Hathaway BJ, Billing DE, Dudley R, Nicholls P. Electronic energy levels and stereochemistry of the cis-distorted octahedral complex nitritobis-(2, 2'-bipyridyl) copper (II) nitrate. *J Chem Soc A Inorg phys theor.* 1969; 1969:1192-1197.
67. Nikles DE, Powers MJ, Urbach FL. Copper (II) complexes with tetradentate bis (pyridyl)-dithioether and bis (pyridyl)-diamine ligands. Effect of thio ether donors on the electronic absorption spectra, redox behavior, and EPR parameters of copper (II) complexes. *Inorg Chem.* 1983; 22(22):3210-3217.
68. Ray RK, Kauffmann GB. An EPR study of copper (II)-substituted biguanide complexes. Part III. *Inorganica Chim Acta.* 1990; 174(2):237-244.
69. Smith DW. Relationship between electron spin resonance g-values and covalent bonding in tetragonal copper (II) compounds. *J Chem Soc A Inorg phys theor.* 1970; 1970:3108-3120.
70. El-Tabl AS. Synthetic and spectroscopic investigations of some transition metal complexes of hydroxy-oxime ligand. *J Chem Res.* 2004; 2004(1):19-22.
71. Symons M. *Chemical and Biological Aspects of Electron Spin Resonance*, New York: Van Nostrand Reinhold Wokingham. 1979.
72. Shieh SJ, Chea CM, Peng SM. A colorless Cu(II) complex of CuO₆ with a compressed tetragonal octahedron, *Inorganica Chim Acta.* 1992; 192: 151-152.
73. El-Tabl AS. An esr study of copper (II) complexes of N-hydroxyalkylsalicylideneimines. *Transit Met Chem.* 1997; 23(1):63-65.
74. Al-Hakimi AN, Shakhdoifa MM, El-Seidy AM, El-Tabl AS. N, N 2-bis (3-(3-hydroxynaphthalen-2-yl) methylene-amino) propyl) phthalamide. *J Korean Chem Soc.* 2011; 55(3):418-429.
75. Shieh SJ, CHE CM, Peng SM. A colorless Cu (II) complex of CuO₆ with a compressed tetragonal octahedron. *Inorganica Chim Acta.* 1992; 192(2):151-152.
76. El-Tabl AS. Synthesis and spectral studies on mononuclear copper (II) complexes of isonitrosoacetylacetone ligand. *Pol J Chem.* 1997; 71(9):1213-1222.
77. El-Tabl AS, Imam SM. New copper (II) complexes produced by the template reaction of acetoacetic-2-pyridylamide and amino-aliphatic alcohols. *Transit Met Chem.* 1997; 22(3):259-262.
78. Gaber M, Ayad MM, Ayad MI. Synthesis, thermal and electrical studies on zirconyl complexes with schiff bases derived from 2-hydroxy-1-naphthaldehyde and some aromatic diamines. *Thermochim Acta.* 1991; 176:21-29.
79. El-Tabl A, Abou-Sekkina M. Preparation and thermophysical properties of new cobalt (II), nickel (II) and copper (II) complexes. *Pol J Chem.* 1999; 73(12):1937-1945.
80. Hall IH, Lee CC, Ibrahim G, Khan MA, Bouet GM. Cytotoxicity of metallic complexes of furan oximes in murine and human tissue cultured cell lines. *Appl Organomet Chem.* 1997; 11(7):565-575.
81. Gaetke LM, Chow CK. Copper toxicity, oxidative stress, and antioxidant nutrients. *Toxicology.* 2003; 189(1-2):147-163.
82. Romero D, Aguilar C, Losick R, Kolter R. Amyloid fibers provide structural integrity to *Bacillus subtilis* biofilms. *Proc Natl Acad Sci.* 2010; 107(5):2230-2234.
83. Huh AJ, Kwon YJ. "Nanoantibiotics": a new paradigm for treating infectious diseases using nanomaterials in the antibiotics resistant era. *J. Control Release.* 2011; 56(2):128-145.
84. Gurunathan S, Han JW, Dayem AA, Eppakayala V, Kim JH. Oxidative stress-mediated antibacterial activity of graphene oxide and reduced graphene oxide in *Pseudomonas aeruginosa*. *Int J Nanomedicine.* 2012; 7:5901.
85. Nagy A, Harrison A, Sabbani S, Munson Jr RS, Dutta PK, Waldman WJ. Silver nanoparticles embedded in zeolite membranes: release of silver ions and mechanism of antibacterial action. *Int J Nanomedicine.* 2011; 6:1833.
86. Wang L, Hu C, Shao L. The antimicrobial activity of nanoparticles: present situation and prospects for the future. *Int J Nanomedicine.* 2017; 12:1227.
87. El-Tabl AS, Abd-El Wahed MM. Synthesis, Structural Investigation and Biological Evaluation of New Metal Complexes of 4, 4-(bis (phenylamino) methylene) bis-(azoanylylidene) Bis (hydroxyimino) pentan-2-one Ligand. *J Chem and Cheml Sci.* 2016; 6(2):109-126.
88. El Saied FA, Abd-Elzاهر MM, Abdou S, Shakhdoifa MM, Rasras AJ. Synthesis, physicochemical studies and biological evaluation of unimetallic and heterobimetallic complexes of hexadentate dihydrazone ligands. *Beni-Seuf Univ J Appl Sci.* 2017; 6(1):24-32.
89. El-table AS, Wassel MA, Arafa MM. Preparation and investigation of fulvic acid and its metal derivative complexes with application. *Int J Sci Eng Res.* 2017; 8:1663-1679.
90. El-Tabl AS, Abd-Elwahed MM, Fahim SH. M. Metal Chelates as Antitumor Agents: Synthesis, Spectroscopic Characterization and Cytotoxic Action of Metal Chelates of New Dioxime Ligand. *J Chem and Cheml Sci.* 2018; 8:1026-1047.
91. El-Tabl AS, Abd-Elwahed MM, El-Saied SA. Design, Spectroscopic Characterization and Antitumor Action of Synthetic Metal Complexes of Novel Benzohydrazide Oxime. *J Chem and Cheml Sci.* 2018; 8:1048-1072.
92. El-Tabl AS, Abd-El Wahed MM, Mosa RM. Novel metal complexes of dehydroacetic acid hydrazone as platforms for hepatocellular carcinoma therapy. *J Chem and Cheml Sci.* 2019; 9(4):128-152.
93. El-Tabl AS, El-Wahed MMA, El-Henawy EM, Abd El-Wahab OE, Hashim SMF. Metal complexes in cancer therapy: Synthesis, spectroscopic characterization and antitumor effect against breast cancer of new dihydroxy phenyl ethylidene amino benzoic acid complexes. *Int J sci eng Res.* 2019; 10(3):631-645.
94. El-Tabl AS, Abd El-Wahed MM, Ashour AM, Abu seta MHH, Hassanin OH, Saad AA. Metallo-organic copper(II) complex in nano size as a new smart therapeutic bomb for hepatocellular carcinoma. *J Chem and Cheml Sci.* 2019; 9(1): 33-44.
95. El-Tabl AS, Shaban MT, Abd El-Wahed NM. Novel Metal Complexes as Antimicrobial Agents, Synthesis and Spectroscopic Characterization. *J Chem and Cheml Sci.* 2019; 9(3):74-108.
96. Akhila JS, Deepa S and Alwar MC. Acute toxicity studies and determination of median lethal dose. *Curr Sci.* 2007; 93:917-920.
97. Tietz NW, Rinker AD, Shaw LM. International Federation of Clinical Chemistry (IFCC) methods for the measurement of catalytic concentration of enzymes. Part 5. IFCC method for alkaline phosphatase (orthophosphoric-monoester phosphohydrolase, alkaline optimum, EC 3.1. 3.1). *J Clin Chem Clin Biochem;* 21:731-748.
98. Wilson K, Walker JM. *Practical biochemistry: Principles and techniques.* Cambridge University Press. 2000.
99. Mazzela FM, Schumacher HR. *Hemoglobin Clinical Chemistry Theory. Analysis and Correlation.* 2010; 40: 771-789.
100. Villanova PA. NCCLS document H18-A: Procedures for the handling and processing of blood specimens. National Committee for Clinical Laboratory Standards. 1990; 24(38).
101. Dickinson B, Unopette WB. *Platelet determination for manual methods.* Rutherford, NJ Becton, Dickinson, and Company. 1996.